Springer

Journal of
Mechanical
Science and
Technology

Journal of Mechanical Science and Technology 22 (2008) 1237~1243

www.springerlink.com/content/1738-494x

Effects of ALR and configuration ratio on turbulent structures in swirling flows

Sam-Goo Lee*

New & Renewable Energy Material Development Center, Chonbuk National University, Jeonbuk, Korea

(Manuscript Received December 4, 2007; Revised March 31, 2008; Accepted April 2, 2008)

Abstract

To assess the significant physics associated with the increase of ALR and configuration ratio of the nozzle tip in pneumatic swirling flows, comprehensive observations using a 3-D PDPA system were experimentally carried out. Profiles of mean velocities, turbulence intensities, SMD variations, and correlations between droplet size and turbulence components were quantitatively acquired. As discussed in a previous literature, axisymmetric swirl angle of 30° is selected for this investigation because of its strong turbulence levels in the flowfield and finer droplet disintegrations. Various ALRs (Air-to-Liquid Mass Ratio) as well as the length-to-diameter ratios of nozzle tip as parameters were chosen. Due to the complex interactions in swirling flows under these variables, this experimental observation will be of fundamental importance to the understanding of turbulence structures. From the observations, it indicated that increasing the ALR causes the spray development to be positively fluctuated on the atomization in both axial and tangential RMS velocities. Also, it can be concluded that the SMD decreases continuously with increase of ALR, substantiating the fact that the fluctuations are inversely proportional to the SMD variation. Meanwhile, the spray behavior is characteristic with a reduction of length-to-diameter ratio; smaller the configuration ratio, the higher the turbulence intensities and smaller SMD variations in the flowfield.

Keywords: ALR (Air-to-Liquid Mass Ratio); PDPA (Phase Doppler Particle Analyzer); Gaussian; SMD (Sauter Mean Diameter); RMS; Configuration ratio

1. Introduction

The optimal designs of swirl flow in gas turbine engine have long been recognized. Applying the best suitable swirl atomizers into the internal combustors provides better mixing enhancement, improves combustion efficiency, and reduces pollution problem. That's why understanding the spray disintegration phenomena in the flowfield from pneumatic atomizers will have a fundamental importance on the ability to characterize the optimum atomizer design. From the practical standpoint regarding this consideration, it is absolutely necessary to have a sharp understanding the prerequisites associated with mean velocity, turbulence levels, droplet diameter, supplied air pressures or ALR (Air-to-Liquid Mass Ratio), and length-to-diameter ratio of the nozzle orifice to meet the requirements of atomization. Atomization from pneumatic atomizers has been investigated extensively for the past decades, in particular, the relationship between droplet diameters and turbulent distributions. In spite of the extensive experimental information for disintegration mechanism by many researchers, the fundamental observations on the spray trajectories are few. Tankin, R. S. and Li, X. [1] investigated experimentally on the spray behavior with and without swirling flows. They pointed out that the strong swirling air improves the mixing of the fuel and air, facilitating the combustion processes.

As it is well known, breaking up the liquid issuing from the pneumatic atomizer into multitudinous small

*Corresponding author. Tel.: +82 63 581 9570, Fax.: +82 63 581 9575
E-mail address: sglee239@chonbuk.ac.kr
DOI 10.1007/s12206-008-0403-z

droplets is to increase the liquid surface area for improving disintegration. In other words, the atomization in two-phase flows is most effectively achieved by generating a high relative velocity between the liquid jet and the surrounding air resulting from higher momentum by the mutual interactions between working fluids. Much of what is known about important parameter affecting the mixing process has been obtained from experiments with air-to-liquid mass flow ratio (ALR) and geometric configuration of the nozzle [2]. The progressive understanding of disintegration process has been achieved in experimental approaches of the swirling turbulent velocity, and improved results were obtained [3, 4]. With the development of laser diagnostics, many experimental investigations on turbulent mixing enhancement have been carried out [5]. Their experimental observations were mainly focused on the 3-D mean velocities, 3-D RMS velocity fluctuations, liquid flux, and SMD, concluding that the air turbulence close to the nozzle could not influence droplet dispersion and, thus, the rate of spread of the spray, which was determined by the initial droplet trajectories after the breakup of the liquid jet and the droplet centrifugal effect due to air swirl.

In an attempt to understand the disintegration mechanism affecting swirl flows, researchers [6-8] measured mean and fluctuating velocities. They showed that the droplet diameter is progressively reduced as the ALR is increased. Kennedy [9] reviewed these studies and pointed out that the SMD changed linearly with the surface tension while the influence of the viscosity was minimized. To study the flow patterns at the spray boundary region, Lee [10, 11] made phase Doppler particle analyzer (PDPA) measurements of the fluctuating quantities and correlations between volume flux and number density. In the experiment, the author showed the results that the smaller droplets are inwardly entrained from the spray boundary.

The present investigation examines the effect of the nozzle geometry and ALR on the disintegration and flowfield development of internal mixing swirl flows using a PDPA system.

2. Experiment arrangement

The nozzle configuration used to establish counterswirling mixing of an axisymmetric jet is schematically shown in Fig. 1. The body of prototype

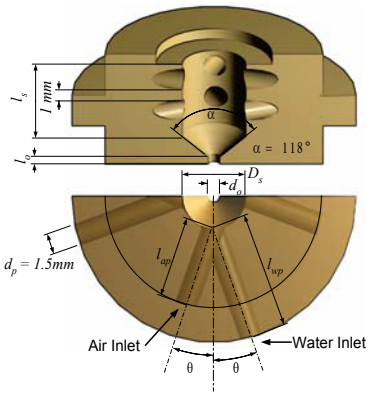

Fig. 1. Specification of nozzle used for the experiment.

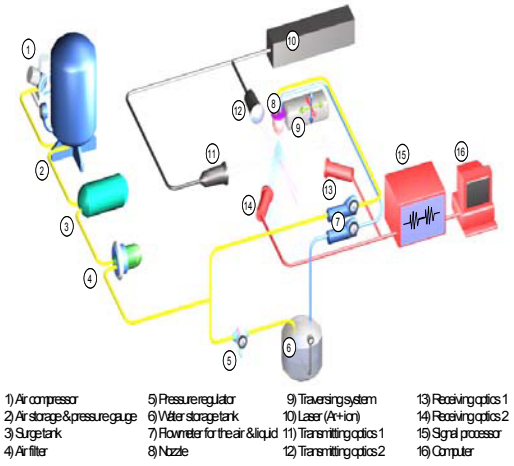

Fig. 2. Experimental setup and diagnostics.

nozzle for generating a counter-flowing spray was fabricated of brass.

The discharge orifice diameter (d_o) is 2mm, swirl chamber diameter (D_s) is 9mm, and the length to diameter ratio of the discharge orifice is 0.65 ($l_o \approx$ 1.3mm). The working fluids were flowed through the tangential ports that results in an angular velocity between two fluids, interacted together in the mixing chamber and injected into the quiescent ambient air at room temperature.

The experimental apparatus is shown schematically in Fig. 2. Continuous and steady flowing water and the pulsation-free air are supplied to the mixing chamber from the pressurized storage tank. Working fluids were properly filtered and regulated. A number of valves, pressure gauges, and flow meters are set up to control the flow rates. Experiments were conducted for the liquid flow rate was kept constant at 7.95g/s

and the air pressures were gradually increased from 20kPa to 200kPa, and ALR can be varied from 0.054 to 0.132. Phase Doppler Particle Anemometer was installed to measure the droplet's behavior of the spray. It provides information on individual particle size between 1μm and 250μm passing through the measurement volume in this investigation. The focal lengths of the transmitting and receiving optics were 400mm and 500mm, respectively. The photo-muitiplier detector voltage of 1400V was optimized to provide the greatest sensitivity, and 45° of scattering was made in the forward direction. Also, bragg cell was used to shift the frequency of one beam by 40MHz to provide directional sensitivity. Data acceptance rate in this experiment was too low for distances less than 20mm from the nozzle exit. Reasons for the low S/N ratio were usually attributed to the presence of non-spherical particles in the PDPA probe volume. Because the PDPA works on the principle of light scattering by spherical particles, signals from non-spherical particles will reject by the instrument. Data acceptance rate varied from 60% to 98% depending on the experimental conditions and the location of the probe volume in relation to the spray geometry. Radial profiles of a geometric sequence space at each measurement locations were obtained at 6 axial positions downstream from the nozzle exit, respectively. The coordinate Z corresponds to the downstream direction at the nozzle exit and y signifies radial outward direction. The measurement volume can be positioned easily at various stations without moving the diagnostic systems in three orthogonal directions by using a computer controlled traversing system that permits positioning to within 0.02mm. The droplet quantities were calculated by collecting 10,000 sample data at each point. The sampling time depends on the local number density of drops, and the 10sec. was set as the upper limit to record data. Precautions for the accurate measurement were taken to avoid possible sources of error during the experiments such as mistracking the particles, nozzle vibrations, and the reading of the flow meters, etc.. Also, the mists of small droplets were discharged to an exhaust system to prevent splashing. To establish the repeatability of the data received, each profile was measured at least twice at different times.

3. Results and discussion

Fig. 3 illustrates the comparisons of normalized axial velocity to establish the effects of ALR regarding axial momentum as a function of Z/do. These data were obtained at various axial stations along the central axis. It is interesting to observe the fact that the maximum velocity in the leading spray (i.e., Z/do= 10) has rather smaller value than that of the downstream axis at a distance of Z/do=15 regardless of the increase in ALR.

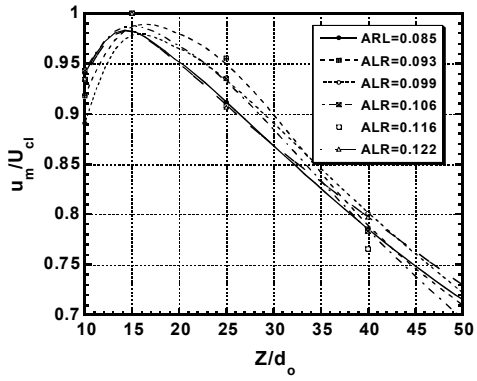

Fig. 3. Non-dimensional variations of axial velocity with various air to liquid mass ratios.

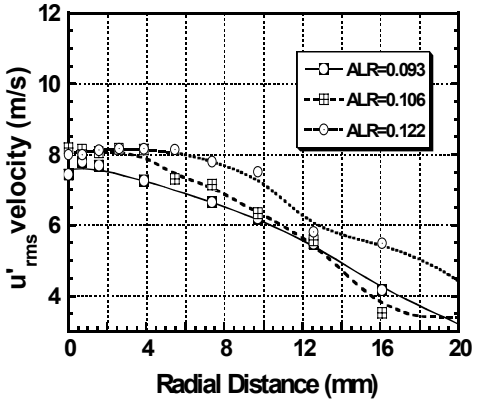

Fig. 4. RMS values of the axial velocity fluctuations with increase of air to liquid mass ratios.

It is also seen that the distributions of mean axial velocity components increase to reach the maximum value of 1 at an axial distance of Z/do and begin to spread toward the jet axis. The reason for this is that the leading droplets at Z/do=10 might be decelerated due to the aerodynamical drag of the surrounding ambient air. Those droplets after this region of Z/do=10 have different aerodynamical interactions, showing a rapid spreading toward the jet axis. This implies that the droplets' overtaking and the velocity acceleration of the leading spray edge may occur.

That's why the droplet maximum velocity develops in the axial distance of Z/do=15. Subsequently, beyond the maximum value at Z/do=15, the axial velocity profile decreases rapidly with increasing Z/do along the downstream locations. Also, it indicates that the profiles of mean axial velocities at sections of Z/do=10-50 can be expressed as a single curve, which illustrates the self-similarity formation or Gaussian profile, as observed by others [12].

Fig. 4 shows the axial velocity fluctuations in terms of radial distances for three representative values of ALR. Since the axial fluctuating velocities before fully developed region do not show an immediate respond to the surrounding air-stream, they propagated with straight trajectories due to the strong axial momentum, as observed in the previous research (Lee, S. G. 2002). Thus, the axial fluctuating components are relatively highest around the central axis even with an increase of ALR. For example, the maximum axial fluctuating velocity for the highest ALR is about 8.3m/s, where the magnitude for the lower case is approximately 7.2m/s. It is also interesting to note that after reaching the highest levels in fluctuation around the center region, i.e., R<4, u'_{rms} steadily decreases and becomes more widening. This shows that the disintegrations in the flowfield with an increase of ALR are still evolving. As expected and evidenced by this absolute values of the velocities, it indicated the positive effects of higher ALR, improving the levels of u'_{rms} in the entire radial section.

Fig. 5 shows the tangential velocity fluctuations in terms of radial distances for three representative val ues of ALR. The spray behavior of w'_{rms} velocity is evidently different from u'_{rms} components as shown in Fig. 4. The development of tangential fluctuating velocity field is apparently important for turbulent dispersion in swirl flows. In accordance with the jet results, the peaks are evidently observed.

The tangential fluctuations are gradually increased from the center to a maximum and then decreased to a local minimum at the outer boundary, substantiating the wider spray width. Increasing the atomizing air causes the spray droplets to fluctuate briskly as shown in Figs. 4 and 5. There is some qualitative similarity even with the increase of ALR as shown in Figs. 4 and 5. But, the quantitative magnitudes are definitely disparate, which can be explained by the higher spreading effect of swirl and ALR. The fluctuation levels of w'_{rms} for the ALR of 0.122 are also higher at whole radial profiles. However, the magnitudes for the lower ALR are gradually decreased, which is reasonably coincident with those of the u'_{rms} velocity distribution. Accordingly, the tangential fluctuations obtain their maximum values in regions at R≈8 where the axial fluctuating velocity gradients become comparatively smaller. In contrast to their slight smaller response in magnitudes for u'_{rm} around the center region (0<R<4), the rms values of w'_{rms} showed larger difference in magnitudes, substantiating the enhanced fluctuation for better atomization due to the higher response of swirl component. Also, near the center region (R<4), the levels of the tangential fluctuating velocities are small, illustrating an opposite phenomenon with those for the axial fluctuating velocities. Meanwhile, the location of the maximum levels

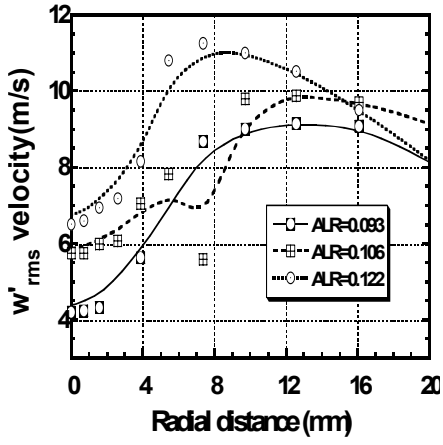

Fig. 5. RMS values of the tangential velocity fluctuations with increase of air to liquid mass ratios.

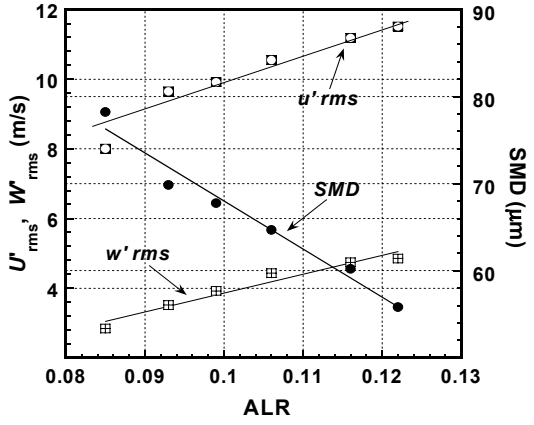

Fig. 6. Comparison of the RMS values for u'rms and w'rms and the SMD as a function of ALR along the center at Z/do=15.

of w'_{rms} is shifted outward from the center at all the cases of ALR. Consequently, it is evident that the spreading trajectories in axial fluctuating velocities with comparative strong axial momentum lead to a reduction of the turbulence levels in tangential directions around the center.

Correlations between RMS values and SMD variation as a function of ALR along the centerline is comparatively plotted in Fig. 6. The both fluctuating velocity quantities are comparatively smaller at lower ALR but steadily increase with an increase of ALR. RMS values of the axial velocity fluctuations have the highest magnitudes at all the cases of ALR when compared to those of tangential fluctuation.

This is mainly because of the strong axial momentum at this axial location as observed in Fig. 3. Meanwhile, the enhanced fluctuating levels are evidently propagated as the ALR is increased, resulting in a more pronounced improvement in atomization. In spite of the upstream location, the SMD decreases rapidly and continuously with increase of ALR. Thus, it can be concluded that the fluctuating components are inversely proportional to the SMD variation. In particular, a linear expression for the correlation of SMD with ALR along the centerline can be predicted: SMD=123.16-551.4 × ALR. But, there is a slight deviation in the expression between SMD and ALR because of its uncertainties during the experiment. The measurement uncertainties of liquid and air supply pressure were ±0.021psig and 0.0043psig respectively with 98% of reliability.

In an attempt to provide understanding the physics in terms of the length-to-diameter ratios (denoted here as l_o/d_o), non-dimensional axial velocity profiles as a function of R/b is shown in Fig. 7. Nozzle configuration ratio is defined as the length to diameter of the final discharge orifice. For the analysis of configuration ratio affecting the flowfield development, nozzle configuration ratios were varied with fixed ALR of 0.106 for the discussion of spray disintegration, having actual values of being 0.15, 0.3, 0.45, and 0.6, respectively. At most of the regions, profile can be approximated by an identical distribution independent of nozzle configuration ratios. It is found to be a general Gaussian in formation on the jet central part.

The velocity distributions near the center (R/b<1) suggest that the velocity self-preserving similarity is evidently established. However, it is interesting to observe that while the droplets are being decelerated progressively near the central region, the velocity in the spray periphery does not acquire a generalized profile but scatters a bit differently. This can be sufficiently explained by taking into account the transfer of momentum from the central region to the periphery due to the inherent swirl and drag. Accordingly, the spray trajectories in the peripheral region are different from the center when compared.

To compare the turbulence level quantitatively, Fig. 8 shows the turbulence intensity with four configuration ratios measured at upstream region of Z/d_o=15. As indicated in this radial profile, the droplet behavior is characteristic with a reduction of length to diameter. At 0.15 of l_o/d_o, while it has the highest turbulence intensities at spray center region of R<10, but it shows comparatively smallest magnitudes of turbulence level at 0.6 of l_o/d_o. Thus, it can be expected to affect the disintegration with an increment of dis-

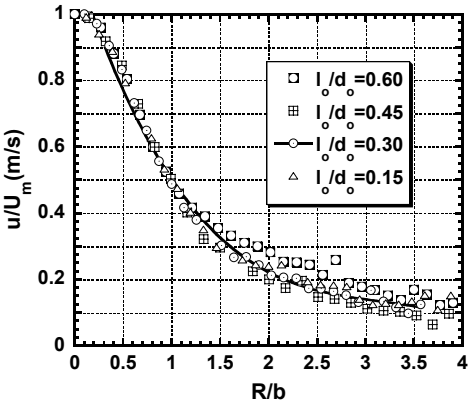

Fig. 7. Non-dimensional axial velocity distribution with configuration ratios at fixed ALR of 0.106 measured at Z/do=15.

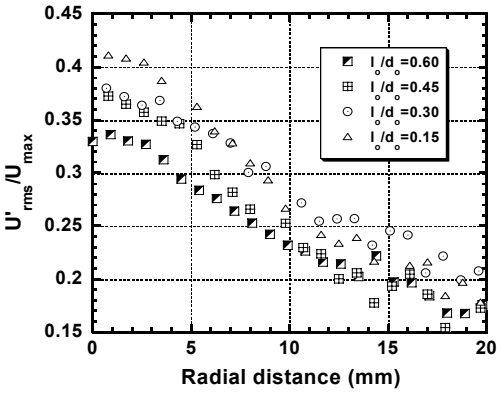

Fig. 8. Distribution of turbulence intensity in terms of configuration ratios at fixed ALR of 0.106.

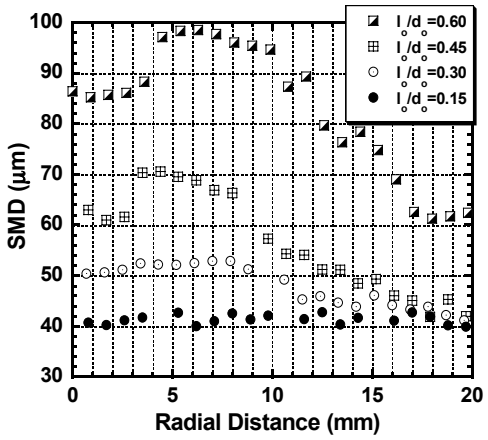

Fig. 9. Distribution of SMD with nozzle configuration ratios at fixed ALR of 0.106.

charge orifice length. Also, Fig. 8 shows that the axial turbulence intensities decrease gradually with increasing radial distances for all the representative configuration ratios. The reason for this can be explained by the rapid spreading in axial direction with higher axial momentum.

Fig. 9 also shows that the mean drop size is reduced remarkably by the decrease of final discharge orifice length at both upstream and downstream axial locations. Fig. 9 shows, more emphatically than others, the effect of l_o/d_o on the global characteristics of the configuration ratio. This contains an important difference between two groups of l_o/d_o; Higher and lower dependence on SMD variation in terms of l_o/d_o. This result is probably due to the influence of discharge orifice length on the turbulent disintegration as observed in Fig. 8. Thus the reduction in SMD with decrease in discharge orifice length may be attributed directly to the shorter breakup regions of the spray that accompanies higher turbulence intensity. Highest value of 0.6 shows a stronger influence on SMD at all radial distances, but the values below 0.6 provide an almost negligible small variation, especially at spray peripheries of R>15. Fig. 9 reveals that the SMD diminishes continuously over the range from 0.15 through 0.6, but the minimum value required for the best performance of atomization was not encountered. Presumably further improvement in atomization performance would be achieved by reducing the length of the final discharge orifice. The spray trajectory of the central region is not susceptible to be affected by the surrounding air and droplet entrainment. Thus, considering the droplet movement in this region is significant feature to be discussed.

4. Conclusions

Experimental parameters such as ALRs (Air-to-Liquid Mass Ratio) and configuration ratios (or length-to-diameter ratio of the final discharge orifice) were considered for analyzing the flowfield development under the selected swirl angle of of θ_s=30°. RMS profiles of axial and tangential velocity variations, correlations between fluctuating components and SMD as a function of ALR, and turbulence intensities were obtained. The objective in this study was to represent the effects of geometric configuration and supplied air pressures on the turbulence flow-field characteristics.

The results obtained that the maximum velocity in the leading spray has rather smaller value than that of the downstream axis at a distance of Z/do=15 regardless of the increase in ALR. Because the leading droplets at Z/do=10 might be decelerated due to the aerodynamical drag of the surrounding ambient air. Also, it indicates that the profiles of mean axial velocities can be expressed as a self-similarity formation or Gaussian profile. Meanwhile, the axial fluctuating velocities before fully developed region do not show an immediate respond to the surrounding air-stream due to its strong axial momentum. But, the tangential fluctuations are gradually increased from the center to a maximum and then decreased at the outer boundary, substantiating wider spray width. Correlations between RMS values and SMD variation as a function of ALR showed that both fluctuating velocity quantities are comparatively smaller at lower ALR but steadily increase with an increase of ALR, resulting in a more pronounced improvement in atomization. Thus, it can be concluded that the fluctuating components are inversely proportional to the SMD variation. In particular, a linear expression for the correlation of SMD with ALR along the centerline can be predicted: SMD=123.16-551.4×ALR. Also, the droplet behavior is characteristic with a reduction of length to diameter: 1) the mean drop size is reduced remarkably by the decrease of final discharge orifice length, 2) Higher and lower dependence on SMD variation in terms of l_o/d_o. Thus, the reduction in SMD with decrease in discharge orifice length may be attributed directly to the shorter breakup regions of the spray that accompanies higher turbulence intensity.

Nomenclature

d_o : Final discharge orifice diameter
d_p : Diameter of passages for the fluids
D_s : Swirl chamber diameter
l_o : Length of final discharge orifice
l_s : Length of swirl chamber
l_{ap} : Length of air passages
l_{wp} : Length of liquid passages
θ_s : Swirl angle of the inlet passages for the fluids
ALR : Air to liquid mass ratio
D_{32} : SMD (Sauter mean diameter)
R : Radial distances
U_m : Maximum axial velocity at the centerline
u'_{rms} : Root mean square of the axial fluctuating component
U : Axial mean velocity
V : Radial mean velocity
W : Tangential mean velocity
Z : Axial distances from the nozzle tip

References

[1] X. Li and R. S. Tankin, Spray Behavior in Non-swirling and Swirling Annular Air Flows, *Atomization and Sprays*, 1 (1991) 319-336.

[2] L. W. Evers, Characterization of the Transient Spray from a High Pressure Swirl Injector, *Atomzation and Sprays*, 4 (1994) 1-10.

[3] K. Ramamurthi and T. J. Tharakan, Experimental Study of Liquid Sheets Formed in Coaxial Swirl Injectors, Journal of Propulsion and Power, 11 (6) (1995) 1103-1109.

[4] A. Mansour and Norman Chigier, 1990, Disintegration of liquid sheets, *Phys. Fluids A*., 706-719.

[5] Y. Hardalupas and J. H. Whitelaw, Coaxial Airblast Atomizers with Swirling Air Stream, AIAA, 30 (4) (1995) 201-232.

[6] S. G. Lee, K. C. Kim, B. J. Rho and K. K. Song, Spray Transport and Atomization in two phase swirl atomizer, *Proceedings of ILASS-Asia*, (2000).

[7] S. G. Lee, B. J. Rho, J. Y. Jung and S. J. Kang, Analysis of Turbulent Flow and Disintegration Characteristics Featuring the Counter-Swirl Pneumatic Nozzle, *4th JSME-KSME Thermal Engineering Conference*, Oct. 1-6, Kobe, Japan, (2001).

[8] M. M. Elkotp, N. M. Rafat and M. A. Hanna, The influence of Swirl Atomizer Geometry on the Atomization Performance, *ICLASS*, (2001) 109-115.

[9] J. B. Kennedy, High number SMD Correlations for pressure atomizers, *Journal of Engrg., for Gas Turbines and Power*, (1986) 191-195.

[10] S. G. Lee and B. J. Rho, Atomization characteristics in pneumatic counterflowing internal mixing nozzle, *KSME International Journal*, 14 (10) (2002) 1131-1142.

[11] S. G. Lee, B. J. Rho and K. K. Song, Turbulent disintegration characteristics in twin fluid counter flowing atomizer., *39th ALAA Aerospace and Sciences Meeting and Exhibit, AIAA 2001-1047*, Reno Nevada, USA, (2001).

[12] N. A. Chigier and A. Chervinsky, Experimental Investigation of Swirling Vortex Motion in Jets, *Journal of Applied Mechanics*, 34 (1967) 443-451.